ADVANCED MATERIALS INTERFACES
www.advmatinterfaces.de

High-Capacitance Nanoporous Noble Metal Thin Films via Reduction of Sputtered Metal Oxides

*Maciej Gryszel, Marie Jakešová, Tomáš Lednický, and Eric Daniel Głowacki**

Increasing the electrochemical surface area of noble metal electrodes is vital for many applications, including catalysis and bioelectronics. Herein, a method is presented for obtaining porous noble metal thin films via reactive magnetron sputtering of noble metal oxides, MO_x, followed by their reduction using chemical reducers or electrochemical current. Variation of reduction conditions yields a range of different electrochemical and morphological properties. This method for obtaining porous noble metals is rapid, facile, and compatible with microfabrication processes. The resulting metallic films are porous and have competitively high capacitance and low impedance.

1. Introduction

Noble metals are remarkable for their catalytic properties, excellent chemical stability, high electrical conductivity, and resistance to formation of native oxide layers.[1,2] Their catalytic properties are exploited for heterogeneous catalysis, for instance, in petroleum processing and catalytic converters on automobiles. As electrocatalysts, they are deployed in fuel cells and electrolyzers.[3] In bioelectronics, noble metals are used as reliable stimulation and recording interfaces for implanted medical technologies like deep brain stimulators, cardiac pace makers, and peripheral nerve interfaces.[4,5] For in vitro biology, they are common materials for biosensor electrodes. In all these applications, high effective surface area is a critical parameter. Roughening or porosification at the nano- and microscale strategies is often employed to yield high interfacial area without sacrificing 2D geometric area.[4,6,7] Common techniques to achieve this include electrochemical etching or electrochemical deposition,[8–10] which leads to nanostructured high-surface-area geometries,[6] orthogonal dissolution of a codeposited metal like silver,[11] or an organic polymer template, to yield porous structures.[12,13] These procedures require multiple steps and materials, and further depend on organic solvents or electrochemical treatments. Electrochemical deposition/etching requires reliable electrical contact to an underlying conductor, and mounting into an electrochemical cell. The goal of this work is to develop a method for high-surface-area noble metal coatings requiring a minimal number of steps to maximize compatibility with high-throughput wafer-scale microfabrication processes. Herein, we detail a general method about how porous/textured Au, Pd, and Pt can be obtained via reactive sputtering of the respective metal oxides, followed by reduction. We find that sputtering with mixed working gases Ar:O_2 yields a (meta)stable oxide, which after reduction produces a conducting surface with remarkable electrochemical capacitance and low impedance. Reactive sputtering with O_2 is a very well-established method for deposition of metal oxide films like Al_2O_3 and TiO_2.[14] Its use for oxides of noble metals, however, is rare.[15,16] In the work, herein we establish this concept generally for reactively sputtered/reduced Au, Pd, and Pt, comparing different reduction conditions and the resulting electrochemical parameters (impedance and capacitance) between these three metals. Overall, the method is straightforward to obtain high electrochemical surface area films in a microfabrication-compatible way. We then use selected optimized reduction procedures to test microelectrodes relevant for bioelectronics applications, demonstrating highly competitive performance in terms of low-impedance electrodes.

2. Results and Discussion

The reactive sputtering/reduction process that we test is performed entirely at room temperature and can be accomplished on arbitrary substrates. The steps are schematized in **Figure 1** for Au; however, the process is analogous for the other metals (all conditions and accompanying scanning electron microscopy (SEM) are shown in the Supporting Information). For the purpose of having appropriate reference samples, we prepare the porous metal films on respective planar Au, Pd, and Pt layers on poly(ethylene terephthalate) (PET) foils. A consistent thickness of the underlying metal (100 nm) is used to ensure a low-resistance contact. The planar metal layers are prepared by sputtering using pure Ar and a low working pressure of 3.8 mTorr to yield films with relatively low roughness. The oxide layers can then

M. Gryszel, E. D. Głowacki
Laboratory of Organic Electronics
Department of Science and Technology
Linköping University
Bredgatan 33, Norrköping 60174, Sweden
M. Jakešová, T. Lednický, E. D. Głowacki
Bioelectronics Materials and Devices Laboratory
Central European Institute of Technology
Brno University of Technology
Purkyňova 123, Brno 61200, Czech Republic
E-mail: eric.daniel.glowacki@ceitec.vutbr.cz
The ORCID identification number(s) for the author(s) of this article can be found under https://doi.org/10.1002/admi.202101973.

DOI: 10.1002/admi.202101973

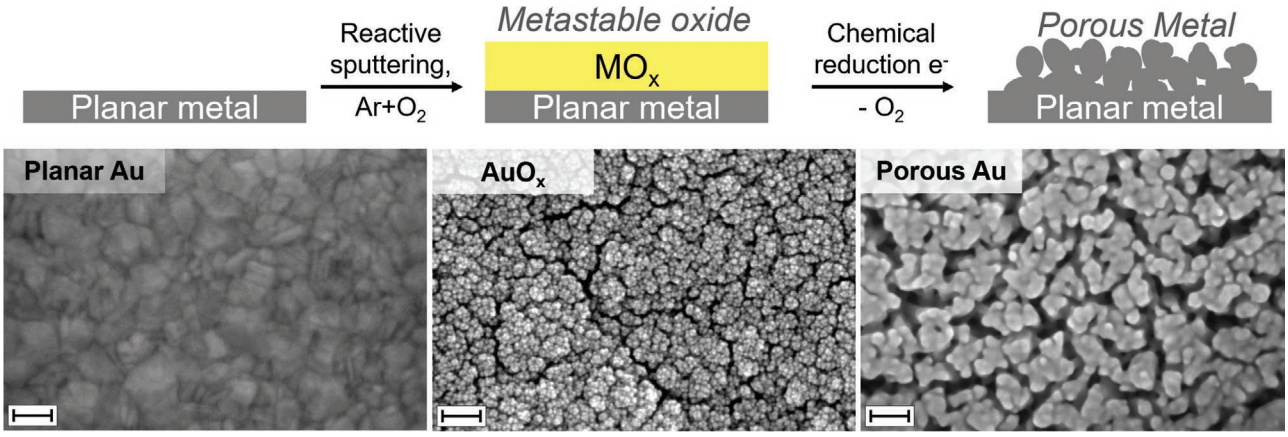

Figure 1. General workflow of the noble metal electrode porosification process, along with corresponding SEM images showing Au as an example. A planar Au film is coated with AuO_x, followed by reduction using *n*-butylamine 1:1 v/v aqueous solution. Scale bar = 50 nm.

be prepared during the same pump down without breaking vacuum. MO_x layers were deposited using an argon/oxygen mixture with a 4:1 Ar:O_2 flow rate ratio. Process details are given in the Supporting Information. Samples were characterized using SEM and with energy-dispersive X-ray spectroscopy (EDX). SEM was used to evaluate the sample morphology and EDX to estimate the metal:oxygen ratio (stoichiometry given in Table S1 of the Supporting Information). Samples were subjected to different chemical or electrochemical (EC) reduction conditions (**Table 1**) and then characterized with electrochemical techniques. Charging–discharging currents in cyclic voltammetry (CV) under deoxygenated conditions were used to calculate electrochemical capacitance (μF cm^{-2}, Table 1). Electrochemical impedance spectroscopy (EIS) measures electrochemical impedance as a function of frequency (**Figure 2**). In all cases, reduced porous samples are compared with planar control samples of the given metals. The impedance of the porous MO_x electrodes is significantly lower than the planar control.

Table 1. Values of electrolytic capacitance. Calculation of capacitance is based on cyclic voltammetry, averaged over 3–4 specimens (corresponding scans are shown in Figure S5 in the Supporting Information). EC: electrochemical reduction; IPA: isopropanol; EtOH: ethanol; and RSD: relative standard deviation.

Sample name	Capacitance [μF cm^{-2}]	
	Average	RSD [%]
Au, EC: –200 μA	214.3	15.8
Au, $nBuNH_2$:water, 1:1	213.0	24.7
Au, IPA	108.7	6.6
Au, IPA_{vapor}	60.8	16.9
Au, 5% H_2 in N_2	78.4	22.5
Au, vacuum, 90 °C	12.0	18.7
Au substrate	31.9	2.1
Pd, ascorbic acid, 0.5 M	416.4	9.4
Pd, EtOH, 60 °C	288.1	7.0
Pd, EC: –200 μA	271.3	9.8
Pd substrate	16.0	22.1
Pt, EC: –0.8 V	1630	3.8
Pt, potassium ascorbate, 0.5 M	1549	4.7
Pt, HCOONa, 0.2 M	408.9	20.2
Pt substrate	14.4	17.5

In our experiments, we have considered both electrochemical reduction procedures and a range of chemical reductants. Electrochemical reduction can be appropriate for obtaining metal electrodes with high capacitance and can be carried out in situ in the given electrolyte. The disadvantage of this method is the restriction to conducting structures, which must be incorporated with an electrochemical cell. In the case of complex multielectrode arrays, controlling electrochemical reduction over many channels can be technically challenging and difficult to reproduce. Chemical reduction, on the other hand, has the advantage that it can be applied uniformly over samples of arbitrary shape and area, including multielectrode devices. In our choice of reductants, we have considered low-cost chemicals, which can be applied at room temperature. Reducing agents can be chosen based on their purity and lack of residues, which could be critical for a high-yield microfabrication process flow. To compare the three metals with each other, we used a consistent thickness of the MO_x film (120 nm) and active area (0.05 cm^2). SEM images of samples before and after reduction procedures can be found in Figures S2–S4 (Supporting Information).

In addition to treatment with chemical reductants, we compared results obtained from electrochemical reduction, which was tested for the three metal oxides, using galvanostatic or potentiostatic conditions. In the cases of AuO_x and PdO_x, galvanostatic reduction yielded the highest-capacitance structures, while potentiostatic reduction worked more optimally for PtO_x. AuO_x affords the widest versatility with respect to selection of a reducing agent, both solution and also gas vapor based. While vapor phase reduction can be easy to implement, we found for all metals that it proceeds slower than solution-phase processes and does not give the best results in terms of electrochemical performance of resultant porous metals. Reduction with H_2 is also possible, by using forming gas (5% H_2 in N_2) at 1 atm. Electrochemical properties and uniformity for forming gas-treated samples were poor, except in the case of Au (see Figure S6

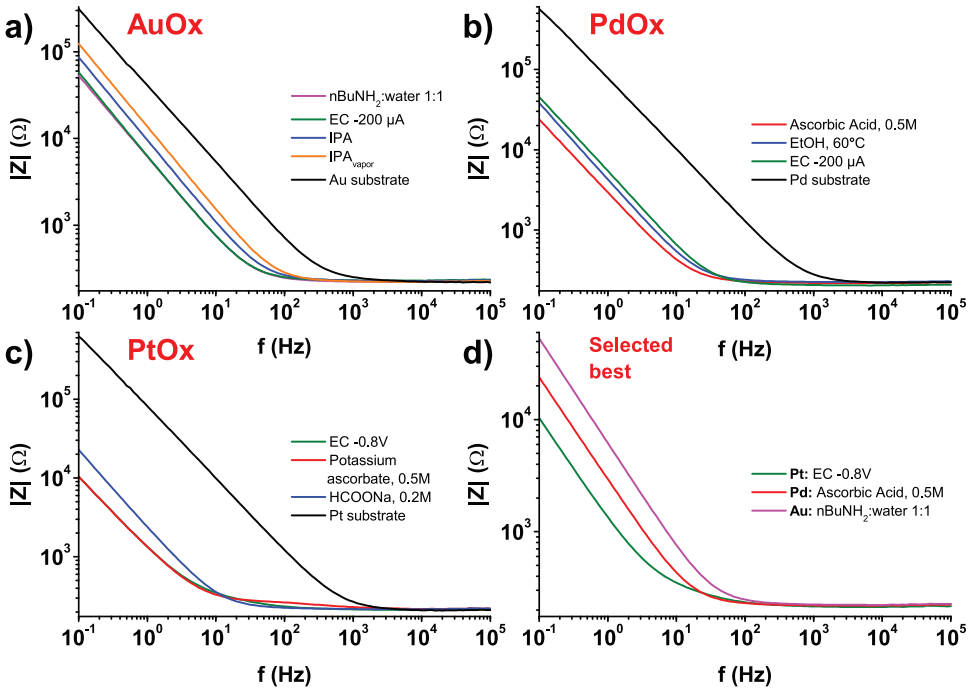

Figure 2. Electrochemical impedance spectra (bode plots) of 0.05 cm^2 electrodes obtained by reduction of a) AuO_x, b) PdO_x, and c) PtO_x. d) The lowest-impedance electrodes for each of the oxides are compared. EC refers to electrochemical reduction, IPA to isopropanol, EtOH to ethanol. Plots shown in the figure are averaged over 3–4 different specimens. Statistics for these data (as relative standard deviation (RSD) for selected frequencies) are given in Table S3 (Supporting Information).

and Table S3 in the Supporting Information). We found that moderate-temperature annealing in vacuum (90 °C) also caused decomposition of AuO_x to form porous Au films.

When we compare porous/roughened samples obtained via reduction of MO_x by their electrochemical performance in terms of low impedance and high electrochemical capacitance; the order from the worst to the best is Au < Pd < Pt. Performance scales with oxygen content remaining in the film following reduction, which may be counter intuitive. Reduced gold samples are essentially completely oxygen free, while platinum retains a relatively high oxygen content. Further, we observe that oxygen-containing samples of reduced PtO_x and PdO_x have higher capacitance and lower impedance when they contain higher oxygen stoichiometry. These favorable electrochemical properties of porous reduced PdO_x and PtO_x can be understood by considering a coexistence of metallic and oxide phases in the films. One may assume that the high apparent oxide content in reduced films, as estimated from EDX analysis, results from a situation where the surface of the sample is fully reduced and metallic, and oxide remains buried in the bulk of the sample. However, such a notion appears incorrect when we consider electrochemical capacitance as a function of film thickness. As shown for the example of potentiostatically reduced PtO_x (**Figure 3**), electrochemical capacitance grows linearly with increased thickness of the sputtered PtO_x precursor. We found the same trend for PtO_x reduced using ascorbic acid or sodium formate, as well as for AuO_x reduced with isopropanol (IPA). These results indicate that the reduced MO_x films can contain relatively homogeneous content metallic and oxide phases, and thanks to suitably high vertical conductivity and substantial porosity, the films behave as volumetric capacitors. Considering the electrical conductivity of the Pd and Pt samples with high residual oxygen content, it is worth noting that Pd and Pt oxides are conductive in their own right. Stoichiometric PdO is a p-type semiconductor.[17] PtO_x is a semimetallic conductor[18] when $x \leq 2$. Therefore, in the case of these porous films, it is not surprising that we are able to achieve low-impedance electrodes. Cross-sectional SEMs (Figure 3c) show that sputtered PtO_x films have a distinct columnular morphology; however, following reduction, the morphology changes to an isotropic sponge-like nanostructure, which is consistent with the thickness-dependent volumetric capacitance behavior measured electrochemically (Figure 3b).

Nanoporous noble metal films are of great interest for microelectrodes for neural recording and stimulation.[10,19] In this application, small geometric area combined with high electrochemical capacitance and low impedance is desired. We have therefore prepared microelectrode arrays (MEAs) with electrodes sized 50 × 50 μm^2, fabricated on the flexible substrate material parylene-c. Parylene-c is employed as both substrate and encapsulant, which is patterned together with Au contact pads and conductive lines using lithography and reactive-ion etching. The microelectrodes themselves were patterned by sputtering metal oxides through a sacrificial parylene-c stencil according to peel-off lithography methods.[20] Photomicrograph images of microelectrode arrays are shown in Figure S7 (Supporting Information). Final devices were obtained by peeling off the sacrificial parylene-c layer and subsequent treatment with the reducer. Details on the fabrication process can be found in the Supporting Information. For microelectrode samples, we carried out the same rounds of

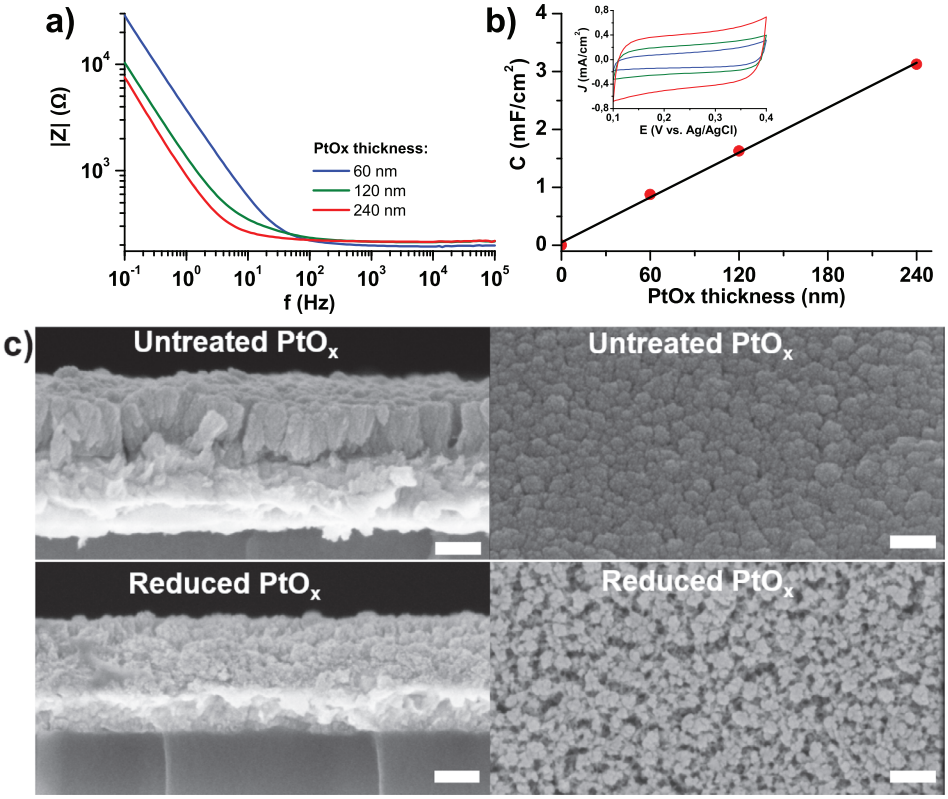

Figure 3. Impact of the as-sputtered untreated PtO_x film thickness on electrochemical properties of the electrode (0.05 cm^2) after potentiostatic reduction (–0.8 V vs Ag/AgCl). a) Electrochemical impedance spectra (bode plots). b) Electrolytic capacitance. The inset shows CV scans used for the capacitance calculation. The color legend is the same as in panel (a). c) Cross-sectional and tilted overview SEMs of PtO_x films as-sputtered (untreated) compared to reduced PtO_x. Scale bars = 100 nm.

reduction conditions detailed in Tables S1 and S2 (Supporting Information), and found that, as expected, the performance of microsized samples follows the same trends as large samples. However, microscaled samples required longer treatment times. In the case of electrochemical reduction, galvanostatic conditions worked better, and larger current densities were necessary than for the 0.05 cm^2 samples. Importantly, we did not observe mechanical stability problems or issues with delamination during the peel-off or reduction processes. We present the results of EIS for porous microelectrodes compared with their smooth sputtered analogs in **Figure 4**. The impedance at 1 kHz for reduced, porous samples drops by a factor of between 8 and 50 times relative to the smooth layers. Porous platinum electrodes have the lowest impedance values overall. With impedance values of 5–10 kΩ at 1 kHz, our 2500 μm^2 porous platinum electrodes are on par or slightly better than the best-to-date reported nanoplatinum microelectrodes (of the same geometrical area),[5] and significantly better than the best-reported sputtered nanoroughened platinum microelectrodes.[19] It should be noted that at high frequency (100 kHz) differences in series resistance are apparent, apparently indicating that porous structures contribute different vertical series resistivity. Stability is critical for any bioelectronics application. We have conducted aging studies in phosphate-buffered saline at 60 °C over over 22 days, and all porous samples retain lower impedance than planar controls (Figure S8, Supporting Information). Porous gold impedance increases over the first few days, approaching stable values of around 3× higher impedance. PdO_x and PtO_x are much more robust, showing only slight changes in impedance over the course of the aging study.

3. Conclusions

Here we have presented a novel method for obtaining porous films of noble metals via reduction of the respective metal oxides. The oxides are prepared by reactive sputtering in an Ar/O_2 mixture. We have designed and tested our method to be compatible with wafer-scale microfabrication processes, and the method is remarkable for simplicity and cleanliness with respect to the introduction of chemical or particulate impurities. The reduction procedures for porosification that we describe should be likewise applicable to noble metal oxides prepared by chemical or electrochemical deposition, or those sputtered from metal oxide targets without the use of reactive O_2. Microelectrodes fabricated using this method achieve competitive values of low electrochemical impedance, and can be particularly promising for microelectrodes used in bioelectronics applications. In terms of impedance and capacitance,

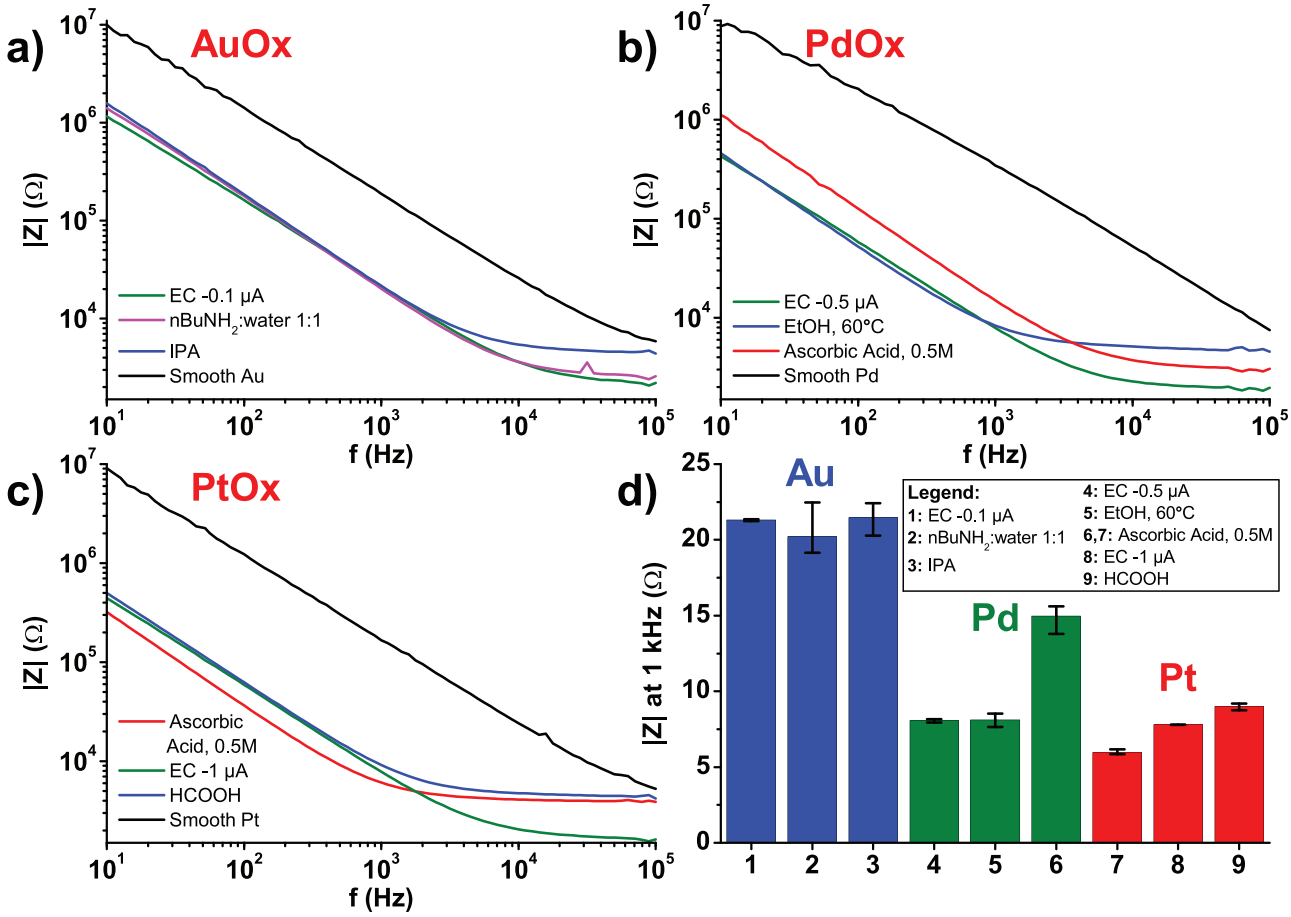

Figure 4. Comparison of electrochemical impedance spectra (bode plots) of the best microelectrodes (50 × 50 µm) obtained by reduction of a) AuO_x, b) PdO_x, and c) PtO_x. d) Values of the absolute impedance at 1 kHz for each of the samples are shown. Results shown in the figure are averaged over 3–6 different specimens ± standard deviation (SD). Smooth layers of Au/Pd/Pt were deposited by sputtering (65 nm at 100% argon, 3.8 mTorr).

the best properties are consistently achieved with PtO_x, even though reduced PtO_x contains more residual oxygen content than gold or palladium films.

Supporting Information

Supporting Information is available from the Wiley Online Library or from the author.

Acknowledgements

The authors gratefully acknowledge financial support from the Swedish Foundation for Strategic Research (SSF); the European Research Council (ERC) under the European Union's Horizon 2020 research and innovation program (Grant agreement No. 949191); funding from the city council of Brno, Czech Republic; and CzechNanoLab Research Infrastructure supported by MEYS CR (LM2018110).

Conflict of Interest

The authors declare no conflict of interest.

Author Contributions

M.G. and E.D.G. conceived the project and wrote the paper with input from all authors. M.G. performed all sputtering experiments, developed all reduction methods, and electrochemistry measurements. M.J. designed and fabricated microelectrodes, assisted with electrochemistry, and performed all lithography. M.G. and T.L. characterized samples using electron microscopy and elemental analyses.

Data Availability Statement

The data that support the findings of this study are available in the supplementary material of this article.

Keywords

electrochemistry, magnetron sputtering, microelectrodes, noble metals, porous metals

Received: October 11, 2021
Revised: December 7, 2021
Published online: January 17, 2022

[1] R. F. Vines, E. M. Wise, *The Platinum Metals and Their Alloys*, The International Nickel Company, New York, NY **1966**.

[2] *Noble Metals* (Ed: Y.-H. Su), InTech, Rijeka, Croatia **2011**.
[3] W. Vielstich, A. Lamm, H. A. Gasteige, H. Yokokawa, *Handbook of Fuel Cells*, John Wiley & Sons, Hoboken, NJ **2010**.
[4] S. F. Cogan, *Annu. Rev. Biomed. Eng.* **2008**, *10*, 275.
[5] C. Boehler, S. Carli, L. Fadiga, T. Stieglitz, M. Asplund, *Nat. Protoc.* **2020**, *15*, 3557.
[6] D. Brüggemann, B. Wolfrum, V. Maybeck, Y. Mourzina, M. Jansen, A. Offenhäusser, *Nanotechnology* **2011**, *22*, 265104.
[7] A. Koklu, R. Atmaramani, A. Hammack, A. Beskok, J. J. Pancrazio, B. E. Gnade, B. J. Black, *J. Phys. D: Appl. Phys.* **2019**, *30*, 235501.
[8] A. S. Nugraha, V. Malgras, M. Iqbal, B. Jiang, C. Li, Y. Bando, A. Alshehri, J. Kim, Y. Yamauchi, T. Asahi, *ACS Appl. Mater. Interfaces* **2018**, *10*, 23783.
[9] C. Li, M. Iqbal, J. Lin, X. Luo, B. Jiang, V. Malgras, K. C. W. Wu, J. Kim, Y. Yamauchi, *Acc. Chem. Res.* **2018**, *51*, 1764.
[10] C. Boehler, D. M. Vieira, U. Egert, M. Asplund, *ACS Appl. Mater. Interfaces* **2020**, *12*, 14855.
[11] Y. H. Kim, G. H. Kim, A. Y. Kim, Y. H. Han, M. A. Chung, S. D. Jung, *J. Neural Eng.* **2015**, *12*, 066029.
[12] F. Kertis, J. Snyder, L. Govada, S. Khurshid, N. Chayen, J. Erlebacher, *JOM* **2010**, *62*, 50.
[13] I. McCue, J. Stuckner, M. Murayama, M. J. Demkowicz, *Sci. Rep.* **2018**, *8*, 6761.
[14] *Thin Film Processes* (Eds: J. L. Vossen, W. Kern) Academic Press, New York, NY **1978**.
[15] Y. T. Lee, J. M. Lee, Y. J. Kim, J. H. Joe, W. Lee, *Nanotechnology* **2010**, *21*, 165503.
[16] L. Maya, G. M. Brown, T. Thundat, *J. Appl. Electrochem.* **1999**, *29*, 881.
[17] H. Okamoto, T. Asô, *Jpn. J. Appl. Phys., Part 1* **1967**, *6*, 779.
[18] H. Neff, S. Henkel, E. Hartmannsgruber, E. Steinbeiss, W. Michalke, K. Steenbeck, H. G. Schmidt, *J. Appl. Phys.* **1996**, *79*, 7672.
[19] B. Fan, A. V. Rodriguez, D. L. Vercosa, C. Kemere, J. T. Robinson, *J. Neural Eng.* **2020**, *17*, 036029.
[20] B. Ilic, H. G. Craighead, *Biomed. Microdevices* **2000**, *2*, 317.